Structure-Based Screening As Applied to Human FABP4: A Highly Efficient Alternative to HTS for Hit Generation

7 AUTHORS, INCLUDING:

Jonas Uppenberg

21 PUBLICATIONS   1,709 CITATIONS

Stefan Svensson Gelius

Swedish Orphan Biovitrum

31 PUBLICATIONS   991 CITATIONS

Tomas Åkerud

AstraZeneca

7 PUBLICATIONS   167 CITATIONS

Mats Wikström

Amgen

36 PUBLICATIONS   1,213 CITATIONS

Structure-Based Screening As Applied to Human FABP4: A Highly Efficient Alternative to HTS for Hit Generation

Maria J. P. van Dongen,*,† Jonas Uppenberg,† Stefan Svensson,†
Thomas Lundbäck,‡ Tomas Åkerud,†,§ Mats Wikström,† and Johan Schultz†

*Contribution from the Structural Chemistry Department and Assay Development and
Screening Department, Biovitrum AB, 11276 Stockholm, Sweden*

Received December 20, 2001

Abstract: The time-limiting step in HTS often is the development of an appropriate assay. In addition, hits from HTS fairly often turn out to be false positives and generally display unfavorable properties for further development. Here we describe an alternative process for hit generation, applied to the human adipocyte fatty acid binding protein FABP4. A small molecular ligand for FABP4 that blocks the binding of endogenous ligands may be developed into a drug for the treatment of type-2 diabetes. Using NMR spectroscopy, we screened FABP4 for low-affinity binders in a diversity library consisting of small soluble scaffolds, which yielded 52 initial hits in total. The potencies of these hits were ranked, and crystal structures of FABP4 complexes for two of the hits were obtained. The structural data were subsequently used to direct similarity searches for available analogues, as well as chemical synthesis of 12 novel analogues. In this way, a series of three selective FABP4 ligands with attractive pharmacochemical profiles and potencies of 10 μM or better was obtained.

Introduction

There exists a vast body of evidence that indicates that elevated plasma levels of free fatty acids provide an important link between obesity, insulin resistance, and type-2 diabetes (for recent reviews, see refs 1−4). Yet it has been observed that mice which are deficient in the adipocyte fatty acid binding protein FABP4, also known as aP2 and A-FABP, lack this link and show increased insulin sensitivity upon dietary obesity.[5] A synthetic small molecule that binds to the human variant of FABP4, thereby blocking the binding of endogenous ligands, is therefore expected to have a similar beneficial effect and might as such be developed into a candidate drug for the treatment of type-2 diabetes.

Today, high-throughput screening (HTS) usually is considered as the method of choice for hit generation in the search for new candidate drugs. Given a particular macromolecular target, an extensive library of diverse chemical compounds, usually comprising 10^4−10^6 entities, is screened for modulators of its biological activity. Hits from HTS subsequently enter an intensive chemistry program in which it is attempted to further develop them into lead molecules with optimized potencies,

selectivities, and pharmacochemical features, and with time into efficient drugs.

An important drawback of HTS is the requirement of a robust assay specific for the target in question. Developing such an assay usually demands much time, because detailed knowledge of the biological function of the target is essential. In addition, the need for a simple read-out of, for instance, a fluorescence or radioactivity signal favors the choice of an indirect assay containing multiple proteins or even complete cells, introducing a considerable risk to detect false positives. For this reason, hits from HTS need to undergo stringent orthogonal tests for confirmation. Finally, it is well documented that difficulties in lead optimization very often can be related to HTS hits that were too big and lipophilic from the beginning.[6,7]

Here we describe the application of an alternative, highly efficient approach to identify novel ligands that preferentially bind to FABP4. This approach, termed structure-based screening, is generally applicable on drug targets as soon as reasonably pure material is available. Moreover, it drastically reduces the risk of false positives and provides high-quality hits with advantageous attributes to enter the hit-to-lead process.

The general idea behind structure-based screening is illustrated in Scheme 1. The process starts with the application of a generic binding assay using a relatively small compound library containing polar compounds of low molecular weight (MW < 350 Da). Nuclear magnetic resonance (NMR) methods

* To whom correspondence should be addressed. E-mail: maria.vandongen@biovitrum.com.
† Structural Chemistry Department.
‡ Assay Development and Screening Department.
§ Biophysical Chemistry Department, Lund University, Sweden.

(1) Boden, G. *Proc. Assoc. Am. Phys.* **1999**, *111*, 241−248.
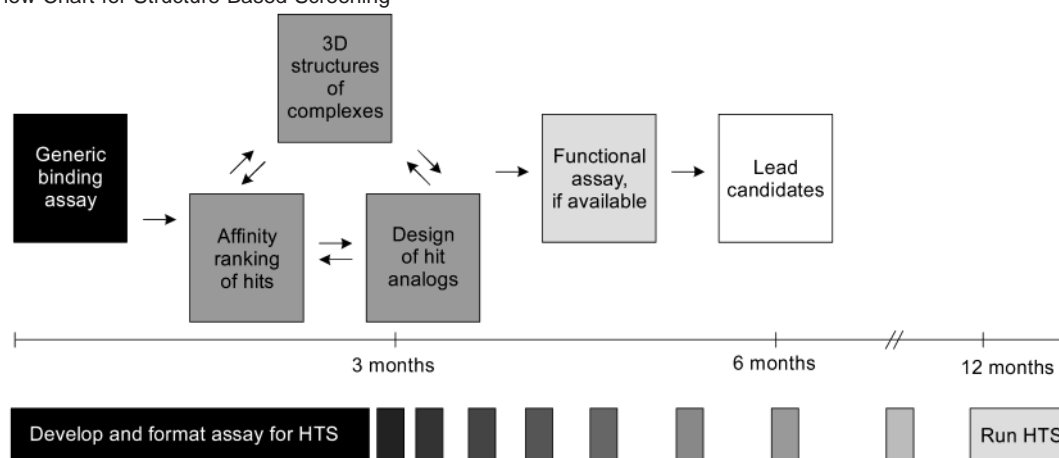(2) Boden, G.; Shulman, G. I. *Eur. J. Clin. Invest.* **2002**, *32*, 14−23.
(3) Lewis, G. F.; Carpentier, A.; Adeli, K.; Giacca, A. *Endocr. Rev.* **2002**, *23*, 201−229.
(4) Arner, P. *Diabetes/Metab. Res. Rev.* **2002**, *18*, S5−S9.
(5) Hotamisligil, G. S.; Johnson, R. S.; Distel, R. J.; Ellis, R.; Papaioannou, V. E.; Spiegelman, B. M. *Science* **1996**, *274*, 1377−1379.
(6) Hann, M. M.; Leach, A. R.; Harper, G. *J. Chem. Inf. Comput. Sci.* **2001**, *41*, 856−864.
(7) Teague, S. J.; Davis, A. M.; Leeson, P. D.; Oprea, T. *Angew. Chem., Int. Ed.* **1999**, *38*, 3743−3748.

Scheme 1. Flow Chart for Structure-Based Screening

are ideally suited for this task.[8,9] A ^{1}H 1D relaxation filter experiment[10,11] applied on a mixture of potential ligands and target protein, for example, combines the quality of being a true and generally applicable binding assay that allows finding low-affinity binders with an adequate throughput. Alternatively, NMR methods such as saturation-transfer difference (STD)[12,13] or WaterLOGSY[14−16] or other biophysical techniques such as size-exclusion separation in combination with mass spectrometry (MS) detection,[17,18] or surface plasmon resonance (SPR),[19,20] could be used to detect small molecule binding to the target.

Next, the hits found in the first step are ranked according to affinity to obtain a crude structure−activity relationship. NMR,[21,22] as well as, for instance, SPR[19,20] or isothermal titration calorimetry (ITC),[23,24] can provide the tools to establish this ranking. In cases where there is a functional assay available that is able to reliably detect weak binders (with affinities down to the millimolar range), it could of course also be used at this stage. On the basis of the resulting hit chart, structure determination efforts on target-hit complexes by means of X-ray crystallography and/or NMR are initiated. Because the hits are

highly soluble, the probability of obtaining crystal structures of target-hit complexes is reasonably high, despite their generally rather low affinity. Hits for which complex structures are determined are prioritized for further development. If no high-resolution structures are obtained, one may have to resort to low-resolution structural information from, for example, epitope mapping by NMR of the binding surface[25−27] or automated docking of ligands.[28,29] The structural data obtained are subsequently used to design new potential ligands with improved binding properties. These new compounds enter the process at the second step, that is, affinity ranking, and are further optimized by structure-based design.

Results and Discussion

Initial Binding Assay. For the initial binding assay, NMR ^{1}H 1D $T_{1\rho}$-relaxation filter experiments[11] were used. Binding of a small molecular ligand to FABP4 results in a reduced tumbling rate of the ligand and consequently an increase in the ligand NMR line widths (and concomitant decrease of the peak amplitudes). In contrast to the SAR-by-NMR method, which utilizes chemical shift changes of protein resonances in either 2D ^{1}H−^{15}N HSQC[30,31] or ^{1}H−^{13}C HSQC spectra,[32] ^{1}H 1D $T_{1\rho}$-relaxation filter experiments circumvent the need to deconvolute active mixtures to identify hits, because the NMR signals of the individual compounds in the mixture are monitored. In addition, experiments which monitor changes in the ligand spectrum do not require any isotope-labeled target protein and are not limited to target proteins below a certain molecular size, as are methods relying on the observation of the signals from the protein. The STD and WaterLOGSY techniques both monitor ligand resonances and therefore possess the same advantages as the ^{1}H 1D $T_{1\rho}$-relaxation filter experiment. The performance of these experiments, which have the additional advantage of requiring smaller amounts of protein, relies on an

(8) Diercks, T.; Coles, M.; Kessler, H. *Curr. Opin. Chem. Biol.* **2001**, *5*, 285−291.
(9) Stockman, B. J.; Farley, K. A.; Angwin, D. T. In *Methods in Enzymology: Nuclear Magnetic Resonance of Biological Macromolecules, Pt A*; Academic Press Inc.: San Diego, 2001; Vol. 338, pp 230−246.
(10) Scherf, T.; Anglister, J. *Biophys. J.* **1993**, *64*, 754−761.
(11) Hajduk, P. J.; Olejniczak, E. T.; Fesik, S. W. *J. Am. Chem. Soc.* **1997**, *119*, 12257−12261.
(12) Mayer, M.; Meyer, B. *Angew. Chem., Int. Ed.* **1999**, *38*, 1784−1788.
(13) Mayer, M.; Meyer, B. *J. Am. Chem. Soc.* **2001**, *123*, 6108−6117.
(14) Dalvit, C.; Pevarello, P.; Tato, M.; Veronesi, M.; Vulpetti, A.; Sundström, M. *J. Biomol. NMR* **2000**, *18*, 65−68.
(15) Dalvit, C.; Fogliatto, G.; Stewart, A.; Veronesi, M.; Stockman, B. *J. Biomol. NMR* **2001**, *21*, 349−359.
(16) Dalvit, C.; Fasolini, M.; Flocco, M.; Knapp, S.; Pevarello, P.; Veronesi, M. *J. Med. Chem.* **2002**, *45*, 2610−2614.
(17) Siegel, M. M.; Tabei, K.; Bebernitz, G. A.; Baum, E. Z. *J. Mass Spectrom.* **1998**, *33*, 264−273.
(18) Moy, F. J.; Haraki, K.; Mobilio, D.; Walker, G.; Powers, R.; Tabei, K.; Tong, H.; Siegel, M. M. *Anal. Chem.* **2001**, *73*, 571−581.
(19) Karlsson, R.; Kullman-Magnusson, M.; Hamalainen, M. D.; Remaeus, A.; Andersson, K.; Borg, P.; Gyzander, E.; Deinum, J. *Anal. Biochem.* **2000**, *278*, 1−13.
(20) Hamalainen, M.; Markgren, P.; Schaal, W.; Karlen, A.; Classon, B.; Vrang, L.; Samuelsson, B.; Hallberg, A.; Danielson, U. *J. Biomol. Screening* **2000**, *5*, 353−360.
(21) Hajduk, P. J.; Dinges, J.; Miknis, G. F.; Merlock, M.; Middleton, T.; Kempf, D. J.; Egan, D. A.; Walter, K. A.; Robins, T. S.; Shuker, S. B.; Holzman, T. F.; Fesik, S. W. *J. Med. Chem.* **1997**, *40*, 3144−3150.
(22) Boehm, H. J.; Boehringer, M.; Bur, D.; Gmuender, H.; Huber, W.; Klaus, W.; Kostrewa, D.; Kuehne, H.; Luebbers, T.; Meunier-Keller, N. *J. Med. Chem.* **2000**, *43*, 2664−2674.
(23) Dalvit, C.; Flocco, M.; Knapp, S.; Mostardini, M.; Perego, R.; Stockman, B.; Veronesi, M.; Varasi, M. *J. Am. Chem. Soc.* **2002**, *124*, 7702−7709.
(24) Ladbury, J. E.; Chowdhry, B. Z. *Chem. Biol.* **1996**, *3*, 791−801.
(25) Weigelt, J.; van Dongen, M.; Uppenberg, J.; Schultz, J.; Wikström, M. *J. Am. Chem. Soc.* **2002**, *124*, 2446−2447.
(26) Gronenborn, A. M.; Clore, G. M. *J. Mol. Biol.* **1993**, *233*, 331−335.
(27) Chen, Y.; Reizer, J.; Saier, M. H.; Fairbrother, W. J.; Wright, P. E. *Biochemistry* **1993**, *32*, 32−37.
(28) Walters, W. P.; Stahl, M. T.; Murcko, M. A. *Drug Discovery Today* **1998**, *3*, 160−178.
(29) Gustavsson, A.-L.; Kihlén, M.; Uppenberg, J. *Ration. Approaches Drug Des.* **2001**, 447−450.
(30) Shuker, S. B.; Hajduk, P. J.; Meadows, R. P.; Fesik, S. W. *Science* **1996**, *274*, 1531−1534.
(31) Hajduk, P. J.; et al. *J. Am. Chem. Soc.* **1997**, *119*, 5818−5827.
(32) Hajduk, P. J.; Augeri, D. J.; Mack, J.; Mendoza, R.; Yang, J. G.; Betz, S. F.; Fesik, S. W. *J. Am. Chem. Soc.* **2000**, *122*, 7898−7904.
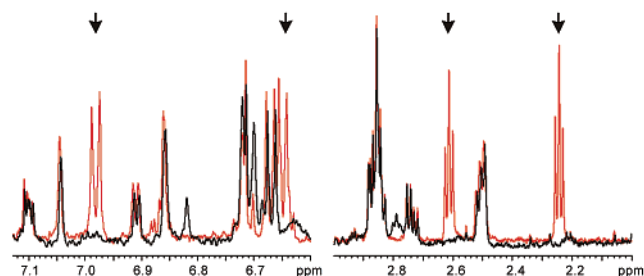
Figure 1. Parts of the aromatic region (left panel) and aliphatic region (right panel) of $T_{1\rho}$-filtered ^{1}H 1D spectra of a cocktail of 10 low molecular weight compounds in the absence (red) and presence (black) of FABP4.

efficient spin diffusion process and improves therefore with increasing molecular weight of the target protein. However, for targets with molecular weights below approximately 20−25 kDa, the sensitivity of these experiments is very low.[15] We therefore used the ^{1}H 1D $T_{1\rho}$-relaxation filter experiment in the FABP4 (14.7 kDa) work.

A library containing 531 compounds, mixed into 57 cocktails, each containing 5−10 compounds, was screened. These compounds were chosen from commercial and internal sources on the basis of a variety of criteria including relatively low molecular weight, high water solubility, and high structural diversity to obtain a broad screening library suitable to screen diverse targets using NMR techniques in a couple of days. The cocktails were designed to avoid spectral overlap and to maximize the chemical diversity within the cocktail.

Figure 1 shows an example of the results for a cocktail containing 10 small molecular compounds. The two doublet signals at 6.64 and 6.98 ppm and the two triplets at 2.25 and 2.62 ppm in the reference spectrum (red) originate from BVT.1960 and disappear when FABP4 is present in the sample. The signals from the nonbinding compounds in the mixture remain unaffected. In total, 52 initial hits were detected for which the signal intensity in the presence of protein was reduced by 80% or more.

Affinity Ranking. A crude structure activity relationship (SAR) for the identified hits can be based on a simple ranking of binding affinities for different ligands. Here we used the ^{1}H 1D $T_{1\rho}$-relaxation-filtered NMR experiment to divide up the hits into two groups. In a ^{1}H 1D $T_{1\rho}$-relaxation-filtered NMR experiment, the integrated signal intensities for the ligand after a spin-lock time with duration SL, $I(SL)$, mainly depend on the fractions of free ligand (pL) and ligand bound to the protein (pLE), respectively, and the corresponding $T_{1\rho}$ values:[33,34]

$$I(SL) = I(0) \exp(-SL/T_{1\rho}) \tag{1}$$

$$\frac{1}{T_{1\rho}} = p_{LE}/T_{1\rho,EL} + p_L/T_{1\rho,L} + p_{LE}p_L(2\pi\Delta\delta)^2 \frac{k_{ex}}{k_{ex}^2 + (2\pi\nu_1)^2} \tag{2}$$

where $\Delta\delta$ is the chemical shift difference for free and bound ligand, k_{ex} is the exchange rate, and ν_1 is the frequency of the spin-lock field.

(33) Lian, L.-Y.; Roberts, G. C. K. In *NMR of Macromolecules: A Practical Approach*; Roberts, G. C. K., Ed.; Oxford University Press: Oxford, 1993; pp 153−182.
(34) Deverell, C.; Morgan, R. E.; Strange, J. H. *Mol. Phys.* **1970**, *18*, 553−559.
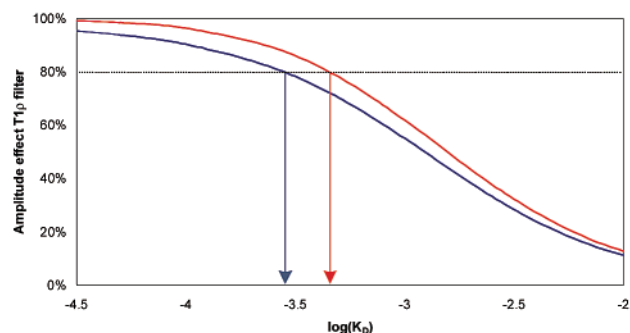
Figure 2. Effect on the amplitudes of the ligand signals (fraction vanished intensity) in ^{1}H 1D $T_{1\rho}$-relaxation filter NMR experiments as a function of affinity according to eq 5. The simulation was performed for an equimolecular mixture of a protein with an average T_2 relaxation time of 79.1 ms and a small molecular ligand with an average T_2 relaxation time of 2 s. The spin-lock field (ν_1) was assumed to be 4000 Hz, and the chemical shift difference for free and bound ligand ($\Delta\delta$) was assumed to be a maximum 50 Hz. The exchange rate (k_{ex}) and dissociation constant (K_D) were estimated assuming a diffusion-controlled "on" rate (k_{on}) of 10^9 s^{-1}. Effects for spin-lock times of 100 ms (blue) and 400 ms (red) were calculated.

If peak amplitudes, $A(SL)$, are regarded, effects due to the transverse relaxation time, T_2, which include substantial exchange terms, play a role as well:

$$A(SL) \propto T_2^* \cdot I(SL) \tag{3}$$

$$1/T_2^* = p_{LE}/T_{2,EL}^* + p_L/T_{2,L}^* + p_{LE}p_L(2\pi\Delta\delta)^2/k_{ex} \tag{4}$$

where T_2^* is the transverse relaxation time corresponding to the observed line width.

Thus, the relative observed effect on the peak amplitudes of the ligand signals in ^{1}H 1D $T_{1\rho}$-relaxation filter experiments upon ligand binding may be written as

$$\text{effect\_}T_{1\rho} = 1 -$$
$$\left\{ \frac{T_{2,L}^* \exp\left(-SL\left(p_{LE}/T_{1\rho,EL} + (p_L - 1)/T_{1\rho,L} + p_{LE}p_L(2\pi\Delta\delta)^2 \frac{k_{ex}}{k_{ex}^2 + (2\pi\nu_1)^2}\right)\right)}{p_{LE}/T_{2,EL}^* + p_L/T_{2,L}^* + p_{LE}p_L(2\pi\Delta\delta)^2/k_{ex}} \right\} \tag{5}$$

Figure 2 depicts a plot of the relative amplitude reduction of NMR signals of small molecular ligands as a function of binding affinity to a protein target with the size of FABP4 (14.7 kDa).[35] The length of the spin-lock time can be selected to detect ligands with different affinities for the target. When longer spin-lock times are used, weaker binding ligands will be detected. From the simulation, it can be seen that using a spin-lock time of 400 ms results in the nearly complete loss of signals for ligands binding with an approximately 0.5 mM affinity or tighter. This attribute was exploited in the initial FABP4 screen.

Applying a ^{1}H 1D $T_{1\rho}$-relaxation filter with a considerably shorter spin-lock time results in a more stringent binding assay, which makes it possible to classify ligands according to binding affinity because the detection cutoff now is approximately 0.25 mM. In this way, the 52 initial FABP4 hits were examined and classified as weaker (14) and stronger (38) binders, respectively. As this experiment was performed on individual compounds instead of cocktails, potential competition effects were elimi-

(35) Constantine, K. L.; Friedrichs, M. S.; Wittekind, M.; Jamil, H.; Chu, C. H.; Parker, R. A.; Goldfarb, V.; Mueller, L.; Farmer, B. T. *Biochemistry* **1998**, *37*, 7965−7980.
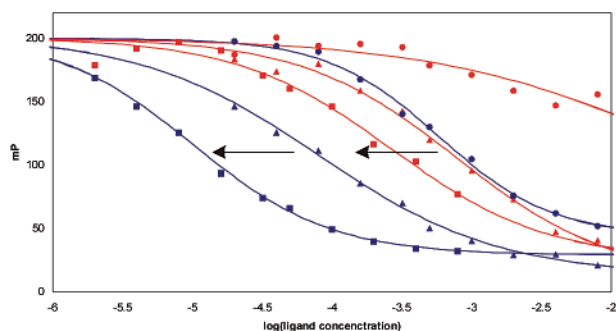
Figure 3. Fluorescence polarization dose−response curves for BVT.1960 and two analogues. Data corresponding to measurements for FABP4 and FABP3 are colored blue and red, respectively. Data points are depicted as ● (BVT.1960); ▲ (BVT.4097); ■ (BVT.1961).

nated as well. The vast majority of the initial hits (43 out of 52, 83%) comprised a CO_2^-, SO_3^-, or PO_3^- group, indicating that they are fatty acid mimics, and this feature was further accentuated in the strong binder category where 95% (36 out of 38) of the hits comprised a CO_2^-, SO_3^-, or PO_3^- group.

The potencies of the highest ranked hits were subsequently measured using a fluorescence polarization assay,[36] which was available in this case. Binding of the fatty acid analogue to FABP4 results in a reduced tumbling rate and consequently an increase in fluorescence polarization. Successive additions of the NMR hits (0.002−4.0 mM) replaced the fatty acid analogue, resulting in a dose-dependent attenuation of polarization signal from which EC_{50} values were deduced. To assess selectivity, potencies of the hits were also measured for FABP3. As an example, the fluorescence polarization dose−response curve for BVT.1960, with an EC_{50} value for FABP4 of 590 ± 60 μM, is shown in Figure 3. This compound was shown to be at least 25 times more selective for FABP4 over FABP3 (EC_{50} = 30 ± 15 mM).

Complex Structures. For two of the ligands revealed by means of NMR, X-ray crystallographic structures of FABP4 in complex with these ligands could be obtained. Figure 4 shows a region of the crystal structure of FABP4 in complex with BVT.1960. As in previously published FABP-fatty acid complex structures,[37−39] the figure reveals the interactions between the carboxylate group of the NMR hit and a conserved tyrosine side chain (Tyr 128). In addition, a novel interaction, not found in FABP-fatty acid complexes, was found for a distal hydroxyl group, which forms a hydrogen bond to the side chain of Asp 76.

FABPs constitute a family of a dozen homologous proteins, expressed in a highly tissue-specific manner. An attractive FABP4 binding compound should not bind (or bind significantly weaker) to other human fatty acid binding proteins, though. In particular, binding to FABP3, which is expressed in heart and muscle, should be avoided. The amino acid sequences of FABP4 and FABP3 are 65% identical[40] with only a few substitutions

(36) Dandliker, W. B.; Hsu, M. L.; Levin, J.; Rao, B. R. *Methods in Enzymology*; Academic Press Inc.: San Diego, 1981; Vol. 74 Pt C, pp 3−28.
(37) Xu, Z. H.; Bernlohr, D. A.; Banaszak, L. J. *J. Biol. Chem.* **1993**, *268*, 7874−7884.
(38) Banaszak, L.; Winter, N.; Xu, Z. H.; Bernlohr, D. A.; Cowan, S.; Jones, T. A. *Advances in Protein Chemistry*; Academic Press Inc.: San Diego, 1994; Vol. 45, pp 89−151.
(39) Reese-Wagoner, A.; Thompson, J.; Banaszak, L. *Biochim. Biophys. Acta- Mol. Cell. Biol. Lipids* **1999**, *1441*, 106−116.
(40) Veerkamp, J. H.; Peeters, R. A.; Maatman, R. *Biochim. Biophys. Acta* **1991**, *1081*, 1−24.
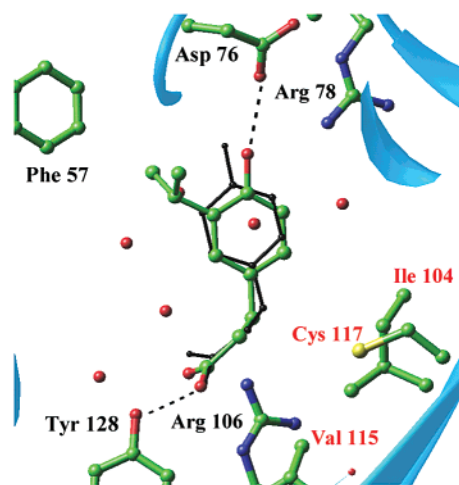
Figure 4. Crystal structure of the ligand-binding site of human FABP4. The structure of the initial hit from the NMR screen (BVT.1960 shown in black) was used to design a higher affinity ligand (BVT.1961 shown in color) with a similar binding mode and retained selectivity against FABP3. Amino acid residues annotated with red labels are different in FABP3 as compared to those of FABP4.

Figure 5. Amino acid sequence alignment of human FABP3 and FABP4.

in the ligand-binding pocket (Figure 5). The FABP4−BVT.1960 crystal structure in combination with a protein sequence comparison reveals that the selectivity of BVT.1960 against FABP3 can be attributed to the effect of V115L and C117L substitutions. Presumably, the additional bulkiness introduced by these substitutions hampers the beneficial van der Waals interactions experienced by one of the flanks of BVT.1960.

Hit Optimization. Because of the >25 times selectivity for FABP4 over FABP3 and the availability of a complex structure, the BVT.1960 scaffold was chosen to be the starting point for the generation of analogues. From the crystal structure, it was found that the flank opposite the one interacting with Val 115 and Cys 117 pointed toward an unoccupied portion of the binding pocket. It was therefore believed that the ligand could be extended into that direction, to improve binding properties. This notion was employed to guide similarity searches in the Available Chemicals Directory (ACD-3D, MDL Information Systems, Inc.) and the Pharmacia compound collection. In total, 11 compounds, four of them commercially available, were checked for improved binding characteristics, both regarding affinity and selectivity against FABP3. As is summarized in Figure 6, it was found that substitutions at the ethylene linker carbons resulted in a loss of selectivity, whereas replacing the *para*-hydroxyl group on the aromatic ring resulted in decreased potency. Substitutions at the *ortho* and *meta* positions with respect to the ethylene linker, on the other hand, appeared to have the capacity to combine improved potency with retained selectivity (Table 1).

On the basis of these findings, 12 additional BVT.1960 analogues, mainly differing in substitutions on the phenyl ring,
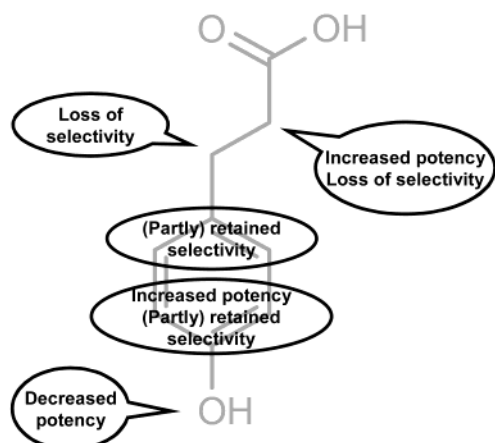
Figure 6. Summary of potency for FABP4 and selectivity against FABP3 of 11 analogues to BVT.1960 from the Available Chemicals Directory and the Pharmacia compound collection.

were synthesized (SINTEF Applied Chemistry, Trondheim, Norway). Binding studies by NMR and fluorescence polarization for these compounds distinctly pointed to a beneficial effect of substitutions at the *meta* (R_2) position (Table 2). As is shown in Figure 3, an ethyl substitution on this position reduced the EC_{50} for FABP4 from 590 to 80 μM. An analogue with an isopropyl substitution, BVT.1961, combined a potency of 10 μM with completely retained selectivity for FABP4. The relative potencies of the methyl, ethyl, and isopropyl analogues suggested that these compounds bind to the same site and in a similar way as the unsubstituted NMR hit. An X-ray structure confirmed that BVT.1961 adopts a binding mode equivalent to that of BVT.1960 (Figure 4).

The binding of BVT.1960 and BVT.1961 to FABP4 was also examined by observing perturbations in $^1H-^{15}N$ correlation experiments. Figure 7 shows the 2D $^1H-^{15}N$ HSQC spectra of ^{15}N-labeled FABP4 in the absence (black) and presence of BVT.1960 (red) or BVT.1961 (green). It can be seen from these spectra that binding of BVT.1960 and BVT.1961 results in the sharpening of a common set of signals, corresponding to amide groups of amino acid residues that define the binding pocket. In the absence of either of these ligands, these amide resonances are extensively exchange-broadened. Chemical shift differences between the resonances of the two complexes are generally small, again indicating equivalent binding modes, with the exception of the Asp 76 amide resonance. As could be confirmed by the X-ray structures of the FABP4 complexes (Figure 4), the substantial chemical shift change of this resonance is due to the short distance between the Asp 76 amide group and the isopropyl group of BVT.1961, which is absent in BVT.1960.

In general, the low-resolution structural information obtained from epitope mapping by NMR of the binding surface makes it possible to identify the ligand-binding site and to confirm that analogous compounds bind with the same binding mode. This would be crucial information in cases where no high-resolution structures of target-ligand complexes can be obtained. With larger target proteins, for which assignments of the backbone resonances are not possible or are deemed too time consuming to obtain, site-selective labeling schemes[25] could be applied to acquire this information.

Concluding Remarks

BVT.1961 amply fulfills the hit criteria that would have been set in an HTS, that is, a binder to FABP4 that combines a moderate potency with a reasonable selectivity. The same is true for two other analogues. Instead of an isopropyl moiety, these compounds incorporate a benzyl or phenone group at the *meta* position (Table 2). Thus, the structure-based screening approach efficiently generated a series of hits for FABP4, providing valuable starting points for the generation of lead molecules.

Recently, another example of the structure-based screening approach was provided by Moy et al.[18] This group used size-exclusion chromatography coupled to electrospray ionization MS as the initial binding assay to verify the interaction of known inhibitors to MMP-1 and to identify novel ligands to RGS4. NMR was subsequently used to check for specific binding, to identify the ligand-binding site, to provide estimates for IC_{50} and K_D values, and, in the case of MMP-1, for structure determination. Unfortunately, no results of the iterative development of the initial hits have been reported yet in this case. The results reported here for FABP4 show that the complete structure-based screening approach indeed provides a valuable tool for the quick identification of novel ligands with specific binding properties comparable to the confirmed hits from HTS.

Apart from the general applicability in early stages of drug development, a clear advantage of the structure-based screening approach is that it starts from small, highly soluble compounds. The identified ligands thus allow for expansion,[6] to generate molecules with optimized affinity and selectivity, without the immediate risk of obtaining drug candidates with disadvantageous bioavailability properties. The generation of structural data of the binding site early in the optimization process furthermore allows synthetic chemistry to focus on the most promising analogues, not only resulting in a highly efficient hit generation process, but also streamlining the following hit-to-lead efforts.
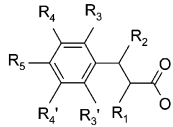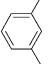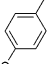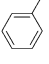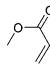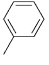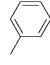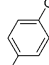
Materials and Methods

NMR Sample Preparation. FABP4 was produced as a recombinant protein from *Escherichia coli* cells harboring a plasmid containing the gene coding for a 132 amino acid protein construct of FABP4. The protein was purified by means of ammonium sulfate precipitation followed by gel filtration using a Superdex 75pg column (Amersham Pharmacia Biotech). Protein concentration and buffer exchange were performed using Millipore Ultrafree-4 centrifugal filters into a buffer containing 50 mM sodium phosphate buffer, pH 7.5, and 5 mM DTT in 100% D_2O.

Cocktails of 5−10 compounds were derived from 500 mM stock solutions of individual compounds in DMSO-d_6. For each cocktail, two NMR samples were prepared, containing 50 μM of each compound in 50 mM sodium phosphate buffer, pH 7.5, in D_2O, in the presence or absence of 50 μM purified protein.
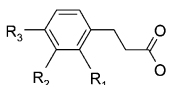
To produce a $^{13}C/^{15}N$-labeled protein, a similar protocol was followed as for the unlabeled protein, except that the *Escherichia coli* bacteria were grown in minimal media containing ^{13}C-glucose and ($^{15}NH_4)_2$-SO_4 as the sole carbon and nitrogen sources. The final protein concentration was 0.2 mM for the samples containing $^{13}C/^{15}N$-labeled protein. The NMR buffer contained 20 mM potassium phosphate, pH 7.6, 2 mM TCEP, 100 μM NaN_3, and 30 μM DSS in 90% H_2O/10% D_2O.
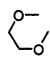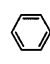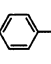
The NMR sample containing $^{13}C/^{15}N$-FABP4 and BVT.1960 was prepared by adding an aliquot of a 73 mM BVT.1960 stock solution in 20 mM potassium phosphate, pH 7.6, 2 mM TCEP to a $^{13}C/^{15}N$-

Table 1. Potencies for FABP4 and Selectivities against FABP3 Derived from the Fluorescence Polarization Assay for Analogues of BVT.1960 As Identified in the Available Chemicals Directory (ACD-3D, MDL Information Systems, Inc.) and the In-House Compound Collection[a]

Analog	#1	#2	#3	#4	#5	#6	#7	#8	#9	#10	#11
R_1	H	H	H	H	[structure]	H	H	H	H	[structure]	[structure]
R_2	H	H	[structure]	[structure]	H	H	H	[structure]	[structure]	H	H
R_3	H	H		H	H	H	H	CH_3	OCH_3	H	H
R_4	H	NO_2	H	H	H	OCH_2CH_3	$C(CH_3)_3/$ $C(CH_3)_3$	H	H	H	H
R_5	NH_2	OH	OH	OH	OH	OH	OH	OH	OH	OH	OH
EC_{50} (μM)	2000	100	2000	1000	100	100	10	100	20	100	100
Selectivity against FABP3	>5	5	>5	0.2	0.5	5	5	0.2	0.5	n.d.	n.d.

[a] Results were obtained semiquantitatively from dose−response experiments.

Table 2. Potencies for FABP4 and Selectivities against FABP3 Derived from the Fluorescence Polarization Assay for Analogues of BVT.1960, Synthesized for the Purpose of Optimizing the Interaction with FABP4

	#1 BVT.1960	#2	#3 BVT.4097	#4	#5		#6 BVT.1961	#7	#8	#9	#10	#11	#12 BVT.1962
R_1	H	H	H	H	H	H	H	CH_2CH_3	$CH(CH_3)_2$	CH_3	H	H	H
R_2	H	CH_3	CH_2CH_3	CH_2CH_3	CH_3	[structure]	$CH(CH_3)_2$	H	H	H	[structure]	[structure]	[structure]
R_3	OH	OCH_3	OCH_3	OH	OH		OH	OH	OH	OH		OH	OH
EC_{50} (μM)	590 ± 60	70 ± 12	> 4000	80 ± 8	260 ± 40	700 ± 300	10 ± 1	270 ± 40	1100 ± 300	1700 ± 800	190 ± 70	5.5 ± 0.7	4.6 ± 0.4
Hill slope	-1.08 ± 0.08	-0.70 ± 0.08	n.d.	-0.67 ± 0.05	-0.91 ± 0.09	-0.63 ± 0.07	-0.88 ± 0.03	-0.77 ± 0.06	-0.81 ± 0.08	-0.61 ± 0.07	-0.68 ± 0.10	-0.73 ± 0.08	-0.92 ± 0.07
Selectivity against FABP3	> 25	3	n.d.	10	9	3	26	7	3	3	4	10	17

FABP4 NMR sample, to reach a final concentration of 60 mM. The $^{13}C/^{15}N$-FABP4-BVT.1961 sample was prepared by adding a 5.7 mM BVT.1961 stock solution in 20 mM potassium phosphate, pH 7.6, 2 mM TCEP to a $^{13}C/^{15}N$-FABP4 NMR sample, to reach a final concentration of 0.7 mM.

NMR Spectroscopy. ^{1}H 1D $T_{1\rho}$-relaxation filter experiments were recorded at 20 °C on a 600 MHz Varian Unity INOVA NMR spectrometer using a 120 μL ^{1}H {^{15}N} flow probe, coupled to a Gilson-215 liquid handler. A set of two experiments with identical experimental parameters was recorded for each cocktail, one in the absence and one
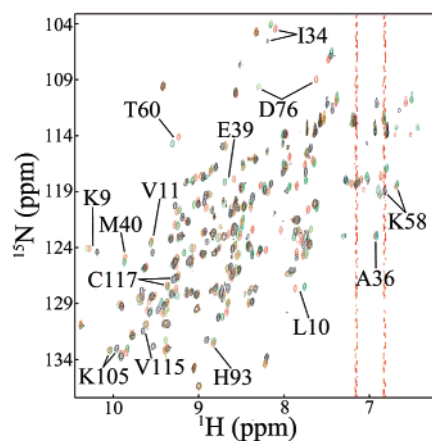
Figure 7. ^1H–^{15}N HSQC of FABP4 in absence of ligand (black), and in the presence of BVT.1960 (red) or BVT.1961 (green). Signals that are substantially shifted or sharpened upon ligand addition are indicated.

in the presence of FABP4. The spin-lock time was set to 400 ms. A second series of experiments, applying a spin-lock time of 100 ms, was recorded for the individual hits. Resulting data were processed and analyzed interactively using the V-NMR software. Compounds that showed a decrease in signal intensities of at least 80% in the presence of protein relative to the reference spectrum were considered as binders.

The two-dimensional NMR experiments were performed at 20 °C on a 800 MHz Varian Unity INOVA spectrometer equipped with a triple resonance ^1H {^{13}C/^{15}N} probe. ^{15}N fast HSQC spectra of ^{13}C,^{15}N-FABP4 in the presence and absence of BVT.1960 and BVT.1961 were recorded with a spectral width of 10 000 Hz sampled over 2048 complex points in ω_2 (^1H) and 2940 Hz sampled over 128 complex points in ω_1 (^{15}N). NMRPipe[41] was used for processing. The spectra were processed using a Lorentzian-to-Gaussian transformation in ω_2 with an exponential line sharpening and Gaussian line broadening of 10 Hz. A cosine bell transformation was used in ω_1. Both dimensions were zero-filled once, and linear prediction to double size was used in ω_2.

Fluorescence Polarization Assay. Triple measurements in a fluorescence polarization assay were performed in 50 mM sodium phosphate, 1 mM EGTA, pH 7.5, and a constant concentration of 2% DMSO. A solution containing 2 mM FABP4 was mixed with 100 nM

fluorophore-labeled fatty acid (C4-BODIPY 500/510 C9, Molecular Probes), after which was added 0.002–4.0 mM NMR hit. The polarization of the fluorescence signal after excitation at 485 nm was measured at 530 nm (Fluorolite FPM-2, Dynex Technologies). Results were fitted in Origin 6.1 with a sigmoidal dose–response function:

$$P = P_{control} + \frac{P_{min} - P_{control}}{1 + 10^{\log(IC50) - \log(LC) \cdot HS}}$$

in which P denotes polarization, LC denotes ligand concentration, and HS denotes Hill slope.

X-ray Crystallography. Crystals of human FABP4 were grown with the hanging drop method. A drop contained 2 μL of protein at 20 mg/mL in 25 mM Tris pH 8.0, 5% DMSO, 1 mM ligand and 2 μL from the reservoir, containing 20% PEG 2000, 5% DMSO, and 0.1 M Tris pH 7.0. Crystals were cryofrozen in mother liquor, and data were collected on a Raxis4 image plate mounted on a Rigaku generator with a rotating copper anode. It was processed with the programs Denzo and Scalepack.[42]

The FABP4 structure was solved by molecular replacement using mouse FABP4 as a model (PDB code: 1lie). Model building was performed with O.[43] The models were refined with Refmac.[44] R_{merge} and completeness were calculated by Scalepack. Refinement R-factors were calculated with Refmac. Model statistics were calculated by Procheck.[45]

Supporting Information Available: A table of the compounds in the cocktail containing BVT.1960, and crystallographic data for the FABP4 in complex with BVT.1960 and BVT.1961 (PDF). This material is available free of charge via the Internet at http://pubs.acs.org.

(41) Delaglio, F.; Grzesiek, S.; Vuister, G. W.; Zhu, G.; Pfeifer, J.; Bax, A. *J. Biomol. NMR* **1995**, *6*, 277–293.

(42) Otwinowski, Z.; Minor, W. *Methods in Enzymology: Macromolecular Crystallography, Pt A*; Academic Press Inc.: San Diego, 1997; Vol. 276, pp 307–326.
(43) Jones, T. A.; Zou, J. Y.; Cowan, S. W.; Kjeldgaard, M. *Acta Crystallogr., Sect. A* **1991**, *47*, 110–119.
(44) Bailey, S. *Acta Crystallogr., Sect. D* **1994**, *50*, 760–763.
(45) Morris, A. L.; Macarthur, M. W.; Hutchinson, E. G.; Thornton, J. M. *Proteins* **1992**, *12*, 345–364.